ELSEVIER

Polymer 43 (2002) 269–277

polymer

www.elsevier.com/locate/polymer

DSC studies on synthesis of superabsorbent hydrogels

H. Omidian*, M.J. Zohuriaan-Mehr

Adhesive & Resin Dept., Iran Polymer Institute (IPI), P.O. Box 14965-115, Tehran, Iran

Received 18 December 2000; received in revised form 5 April 2001; accepted 1 August 2001

Abstract

Reaction scheme of acrylic-based superabsorbing polymers was monitored by a differential scanning calorimeter. Differential scanning calorimetry (DSC) was used to study the heat effects during the polymer synthesis in DSC pan as a micro-scale reactor. Two distinct observations, i.e. inhibition period (IP) and onset of gel formation were recorded during polymerization. The effect of reaction temperature and initiator ($K_2S_2O_8$) concentration was assessed on these general observations. It was found that unrestricted access of the reaction mixture to oxygen and unrestricted loss of water could complicate the polymerization behavior of sodium acrylate in aqueous system. A conceptual kinetic approach was followed to describe the complex process. Finally, DSC observations were compared with their corresponding bench-scale figures. © 2001 Published by Elsevier Science Ltd.

Keywords: Superabsorbent synthesis; Differential scanning calorimetry; Poly(sodium acrylate)

1. Introduction

Superabsorbent polymers are hydrophilic polymers with the ability to absorb large quantities of pure water, saline or physiological solutions [1]. These advanced materials have already been well established in special applications such as consumer care products [2,3] and agriculture [4], and are developing rapidly for the new fields of industrial applications [5]. Acrylamide, acrylic acid and salts of the acid are the common monomers used for the synthesis of the crosslinked absorbing polymers [1]. The monomers can be polymerized either by solution or inverse suspension techniques. In our previous publications [6–12], we explored several aspects of superabsorbent preparation and properties including ultimate capacity for absorbing water, swelling kinetics and its dependence on the synthetic process, monomer and initiator concentration as well as particle size and salinity.

Of the two polymerization techniques, the solution method is preferred industrially for economic reasons and for its simplicity. In this process, pre-heated aqueous solutions of monomers and of crosslinking agent and initiator are prepared separately, brought together in a nozzle-type mixer, and spread on an endless conveyor belt [13] and allowed to react. The reaction mixture is not agitated in anyway, and is occasionally open to the air, providing unrestricted access to oxygen and loss of the solvent (i.e. water) vapor. In addition, the monomers are not usually freed from the enclosed inhibitor and used as manufactured. Although these conditions simplify the process practically, they complicate it very much and the polymerization system is theoretically too complex to be readily investigated through the usual approaches.

In one of our previous works [11], i.e. a bench-scale simulation of the industrial solution process to make superabsorbents, the effect of the bath temperature and initiator concentration were assessed in the presence of evaporative water loss and of oxygen. We observed a retardation period, which primarily attributed to oxygen participation in the polymerization reaction, and extensive losses of water, which seriously affected the final water absorbency of superabsorbent products. To obtain more insight into the events at the point of gel formation, we designed a number of micro-syntheses studied by differential scanning calorimetry (DSC). This was done based on the fact that any exothermic (e.g. polymerization, curing, swelling) as well as endothermic phenomenon (like evaporation) could potentially be monitored by this instrumental method in an exact manner.

This thermal technique has been employed to study kinetics and mechanisms of several polymerization reactions [14], specially those involving crosslinking [15], e.g. curing of epoxy [16–20] and polyester [21,22] resins, phenolic resins [23], vinylic/epoxy resins [24–26],

---

* Corresponding author.

E-mail addresses: h.omidian@proxy.ipi.ac.ir (H. Omidian), m.zohuriaan@proxy.ipi.ac.ir (M.J. Zohuriaan-Mehr).

0032-3861/02/$ - see front matter © 2001 Published by Elsevier Science Ltd.
PII: S0032-3861(01)00546-8

thermosetting polycarbonate [27], and hydrogels like crosslinked poly(2-hydroxyethyl methacrylate) [28]. Study of polyurethane synthesis [29], and in situ polymerization behavior of bone cements [30] are among DSC applications. In nearly all these systems, there is no evaporative component (e.g. solvent) to be removed during the reaction. Moreover, the reactants are mostly purified, and the reactions are run under an inert gas away from air. So, similar kinetic approaches have been used in all the mentioned studies [14–29]. However, in our simulation studies using DSC, the convenient kinetic models cannot be used due to the above-mentioned complexity and uncertainty of the interacting system. Therefore, we tried to make descriptive elucidation for the events during complicated industrial synthesis of superabsorbents via a micro-synthetic approach using DSC.

2. Experimental

2.1. Materials

Acrylic acid, *N*,*N*′-methylenebisacrylamide and sodium hydroxide were supplied from Merck and used as received without any further purification. Potassium peroxydisulfate was recrystallized twice from distilled water (10 ml/g) and dried at 50°C in a vacuum desiccator.

2.2. Instrumental

DSC (Polymer Laboratories) was used for all the syntheses throughout the work using standard aluminum pan in air.

2.3. Measurement of water evaporating rate

A mixture containing all the reaction components except the initiator was prepared in a pre-weighed 100 ml beaker. To fast-reaching bath temperatures, the loaded beaker was pre-heated up to a given temperature (70, 75, 80, 85, 90, 95°C) using hot plate and then immersed in a thermostated water bath at the same temperature. The beaker was quickly re-weighed after 4 min time intervals. Fig. 1 shows the normalized weight-loss data against the time of heating. It should be pointed out that at 90 and 95°C (especially after heating for more than 12 min), few tiny solid particles were separated from the concentrated solution, especially during the short period of each weighing performed at room temperature. This means at these conditions (temperature: 90 and 95°C, time > 12 min), the solution was in a supersaturation state.

2.4. Micro-synthesis in the case of initiator concentration

First, sodium hydroxide (2.51 g) was diluted with prescribed amount of doubly distilled water (4.30 g), under mild agitation and ice cooling, until a clear cold solution was obtained. The latter was poured dropwise onto the acrylic acid (4.40 g), while ice cooling. The crosslinker, methylenebisacrylamide (0.0067 g) was added into doubly distilled water (1.43 g), under shaking, until a clear solution was obtained. The latter solution was added to the neutralized acrylic acid solution. The initiator solution (0.0043–0.0616 g in 2 g water) was similarly prepared as the crosslinker solution, then it was added to the combined solutions of crosslinker and monomers. A sample of about 10–15 mg of this original formulation was withdrawn by a disposable syringe and put into DSC pan at room temperature.

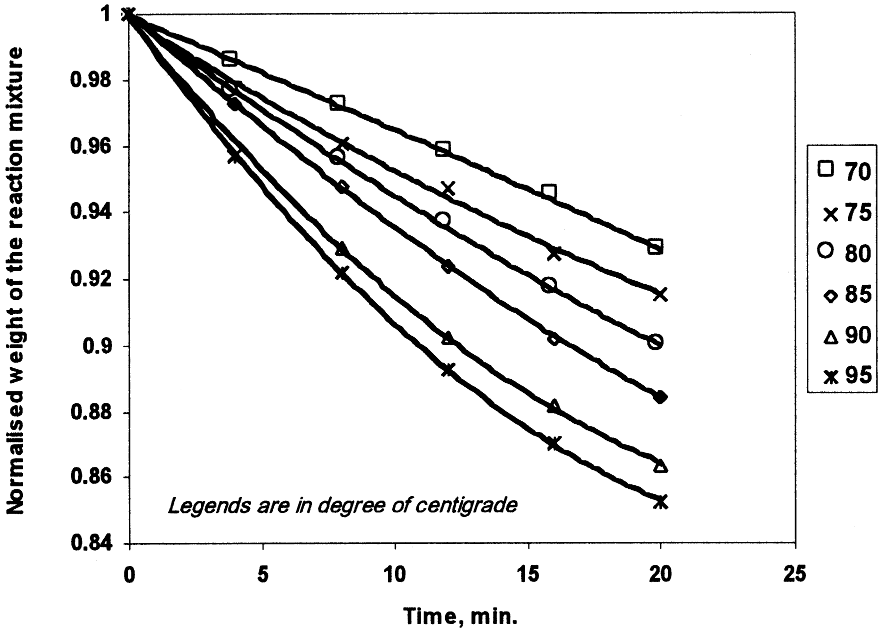

Fig. 1. Normalized weight of the reaction mixture versus heating time at different temperatures.

The pan was quickly put into the DSC heating chamber, again at room temperature. The chamber was closed and heating rate was set at 40°C/min to attain an isothermal reaction, with the least delays to reach a setting temperature. The total period of reaction was 1 h. The polymerizations were carried out under normal atmosphere and at constant temperature of 80°C.

2.5. Micro-synthesis in the case of temperature

Repeat of initiator series, *except* that 0.0118 g of potassium persulfate was diluted with 2.0 g water and used as the initiator solution, and that the temperature was set at 70, 75, 80, 85, 90 and 95°C.

3. Results

An overall common feature of all the micro-syntheses DSC thermograms is shown in Scheme 1 that introduces four distinct regions.

3.1. Initiator case

The first region on the thermograms (A → B) relates to the heat transfer into the contents of the DSC pan to reach them to their set temperatures. This region that was observed within the time range of 0–2 min can be seen as an endothermic peak and was the same for all the reaction mixtures until they reached their set temperatures. The first region was followed by a long and nearly straight region (B → C) (slope 0.35 mcal/s^2). The time range for this process was 10–12 min (see Table 1). A small difference in the shape of the thermograms was observed through the whole range of the initiator studied. One thing was common for all the thermograms. There was a small variation in the slope of the curves through the whole time interval of this region. Rate of heat transfer was ignorably variable (not appeared as a straight line or constant) in this time region for each individual. At low initiator concentration in the range of 0.014–0.076 mol% to monomer, a very weak, wide exothermic peak was observed within the mid-way of the second region. But, at high initiator concentration in the range of 0.091–0.210 mol% to monomer, this weak exothermic peak immediately followed the general endothermic peak within the time interval of 2–3 min. This peak appeared at its most intense form for the highest initiator concentration. The second region was not continued in this way. Through the time range of 12–15 min, a sudden and a very sharp exothermic peak followed this relatively straight region. This was the third region (C → D region), which was observed on the thermograms. But, this peak appeared at different times and shapes. With the initiator range of 0.014–0.029 mol% to monomer, this peak appeared for longer time, but it was stronger. Time and intensity of the peak was decreased through the rest of the initiator range, so that with the highest initiator concentration, no peak was observed in this region. On the other hand, this exothermic peak was accompanied with temperature rise within the reaction mixture. Rise in temperature was higher for the lower initiator concentrations in the range of 0.014–0.034 mol% to monomer and was nearly low and constant for the initiator range of 0.064–0.210 mol% to monomer.

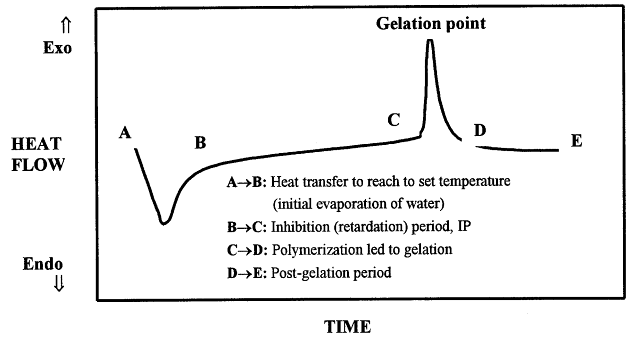

Scheme 1.

Through the time range of about 16–20 min, the fourth region (D → E) was observed as a plateau for all the samples.

3.2. Temperature case

DSC traces in the temperature series of experiments are given in Fig. 2. After reaching the set temperature, thermograms were changed in shape and smoother region was observed. This region appeared at different times and slopes. The longest time (20.4 min) and lowest slope (0.15 mcal/s^2) was observed for the lowest temperature and vice versa (6.12 min for 1.66 mcal/s^2). The shape of the thermograms was not exactly as a straight line, i.e. the rate of heat transfer was not constant through this region (Fig. 2). Small rise in slope of the line that resembles a very weak exothermic peak can be seen for all the individuals, but in different nature. This peak was shifted to shorter times with the increase in temperature, so that it appeared as a shoulder for the high temperature extreme. At the end of this period, an exothermic peak suddenly appeared, the position of which was dependent on the end of the second period for each individual. The highest exotherm was observed for low temperature system (see Table 2). Through the temperature range of 85–95°C, intensity of this exothermic peak was much weaker, but nearly similar. A plateau region for all the individuals followed the exotherm peak.

4. Discussion

Four observed regions in DSC thermograms were shown in Scheme 1. The first region (A → B), which appeared as an endothermic peak, is not chemically important. It was followed by another region (B → C), through which the length and slope of the curve was varied. Such a retardation period is observed in temperature–time profiles reported

Table 1
DSC results and calculated data obtained from superabsorbent micro-synthesis at 80°C in solution with different initiator concentration (initial monomer concentration of 38.48 wt%. q_{instr}, Q_{instr}, Q_{water}, and WL_{IP} are introduced in the text)

Expt.	Initiator amount (g)	$([I]/[M]) \times 100$	IP[a] (min)	WL_{IP} (wt%)	MCg[b] (wt%)	te[c] (min)	Te[d] (°C)	WL_{Te}[e] (wt%)	q_{instr} (cal/g)	$-Q_{\text{water}}$ (cal)	$-Q_{\text{instr}}$ (cal)	$-\Delta H_{\text{Rxn}}$[f] (kcal/mol)	ER[g] (%)
1	0.0043	0.014	13.66	7.14	41.43	1.34	82.08	0.98	− 36.79	0.032	0.371	9.06	56.6
2	0.0062	0.020	14.50	7.56	41.62	1.30	81.72	0.96	− 25.73	0.031	0.256	6.51	40.7
3	0.0088	0.029	14.40	7.51	41.60	1.00	83.67	0.81	− 30.63	0.027	0.310	7.51	46.9
4	0.0100	0.033	12.84	6.73	41.25	0.86	82.29	0.74	− 18.63	0.024	0.181	4.78	29.8
5	0.0104	0.034	13.97	7.30	41.50	0.83	81.74	0.72	− 14.30	0.024	0.145	3.76	23.5
6	0.0197	0.064	12.32	6.47	41.14	0.83	80.95	0.72	− 7.30	0.023	0.072	2.21	13.8
7	0.0235	0.076	12.38	6.50	41.15	0.86	80.76	0.74	− 6.02	0.025	0.061	1.92	12.0
8[h]	0.0280	0.091	12.01	6.32	41.07	1.35	80.11	0.98	− 1.71	0.033	0.017	1.12	7.0
9[h]	0.0410	0.137	11.81	6.22	41.03	1.01	80.24	0.81	− 1.89	0.027	0.019	1.05	6.6

[a] Inhibition (retardation) period.

[b] Monomer concentration just before gelation point.

[c] Duration related to the exotherm peak.

[d] Temperature recorded during the exotherm.

[e] Water lost at Te during te.

[f] Heat of reaction at gelation point.

[g] $\text{ER} = (\Delta H_{\text{Rxn}}/\Delta H_{\text{ref}}) \times 100$; $\Delta H_{\text{ref}} = -16.0$ kcal/mol.

[h] Immediately after the endothermic peak, another wide weak exothermic peak was appeared (at *IP* ~ 2.5 min), but according to the figures for temperature rise, the exothrerm at *IP* ~ 12 min is more probable.

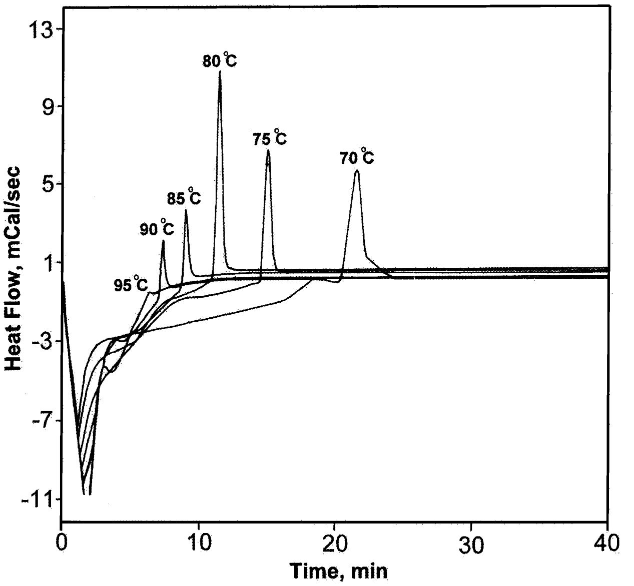

Fig. 2. DSC thermograms in the case of temperature series of experiments.

recently by Chen and Zhao [31,32] although they have not mentioned the scientific concept and meaning of the period.

As we have briefly mentioned [11], the period is due to the presence of oxygen. In this retardation period, although the persulfate ion thermally dissociates (Eq. (1)), this radical initiator as well as the growing chain end radical (Eq. (2)) can be trapped temporarily by oxygen that acts as a free radical scavenger (Eq. (3)). The most probable reaction of molecular oxygen, as shown by Barnes [33] and Bamford [34], may be the formation of a copolymer with the monomer (M), i.e. a polyperoxide (Eq. (4)):

$$S_2O_8^{2-} \xrightarrow{k_1} 2SO_4^{-\cdot}\ (I^{\cdot}) \qquad (1)$$

$$I^{\cdot} + M \xrightarrow{k_2} RM^{\cdot} \qquad (2)$$

$$RM^{\cdot} + O_2 \xrightarrow{k_3} R\text{–}O\text{–}O^{\cdot} \qquad (3)$$

$$R\text{–}O\text{–}O^{\cdot} + M \xrightarrow{k_4} R\text{–}O\text{–}O\text{–}M^{\cdot} \qquad (4)$$

$$RM^{\cdot} + M \xrightarrow{k_5} RM\text{–}M^{\cdot} \qquad (5)$$

This reaction may compete with the addition of the normal polymer radical ($RM^{\cdot}$) to the monomer (Eq. (5)). Since the addition of monomer to the peroxy radical ($ROO^{\cdot}$) is much slower than to $RM^{\cdot}$ ($k_4 \ll k_5$), an inhibition or retardation period is often observed. At the same time in the region B → C (Scheme 1), the temperature of the reaction mixture was sufficient to evaporate water from the system that was open to atmosphere. So, this region was more precisely regarded as the evaporation and inhibition region.

4.1. Water-loss determination and calculation of ΔH_{Rxn}

Water evaporation occurs during the IP and also during the polymerization period (te). Water evaporates (up to 7.5 wt%) more during the IP than the polymerization period. As a result, the monomer concentration increases as much as 3% (Tables 1 and 2, MCg values). With lower initiator amount, the monomer concentration increase was measured to be higher than that of the higher initiator amount, due to higher water lost corresponding to the longer IP. The water lost values (WL_{IP}) were determined based on a series of blank experiments for measuring the rate of water elimination from the reaction mixture (including all the same reaction components except that initiator) at various temperatures. As shown in Fig. 1, the water-lost trends were found to follow approximately linear variations except in the case of temperatures 90 and 95°C. The reason for nonlinearity at higher temperatures may be attributed to higher rate of evaporation at early minutes. By the time, water from the reaction mixture is removed slower since the mixture is more thickened.

WL_{IP} values were used to calculate the amounts of required heat to evaporate water during IP. During the short period of polymerization (te in Tables 1 and 2), the reaction heat (Q_{water}) is partially consumed for evaporating a small part of the residual water (WL_{Te} values) at the corresponding temperatures recorded during the exotherm (Te). Summing up Q_{water} with the heat value obtained from the instrumental data (Q_{instr}) may lead to the real heat of polymerization reaction (ΔH_{Rxn}) at the gelation point according to the following equations:

$$\Delta H_{Rxn} = 0.244 Q_{tot}/M_{pan}\ (\text{kcal/mol}) \qquad (6)$$

$$Q_{tot} = Q_{instr} + Q_{water} \qquad (7)$$

$$Q_{instr} = (1 - 0.01 WL_{IP}) M_{pan} q_{instr} \qquad (8)$$

$$Q_{water} = -13.278\, \Delta H_{vap}\, M_{g(water)}\, WL_{Te} \qquad (9)$$

$$M_{g(water)} = M_{i(water)}(1 - 0.01\ WL_{IP}) \qquad (10)$$

where Q_{tot} is the actual total heat evolved corresponding to the M_{pan} values at gelation point (cal), M_{pan}, the initial weight of total DSC pan content (g), Q_{instr}, the overall heat evolved at gelation point (cal), Q_{water}, the heat consumed for water evaporation at gelation point (cal), q_{instr}, the exotherm at gelation point as recorded by instrument (cal/g), $M_{g(water)}$, the residual water in DSC pan just before gelation point (g), $M_{i(water)}$, the initial weight of total water content in DSC pan, ($M_{i(water)} = 0.601 M_{pan}$) (g), WL_{IP}, the wt% of water loss at given temperature during IP, WL_{Te}, the wt% of water loss at given temperature during the exotherm peak (gelation).

ΔH_{vap} values (enthalpy of vaporation of water at Te, kJ/mol) were obtained using the equation of $\Delta H_{vap} = -0.0497T\ (°C) + 45.376$ resulted from ΔH–T values reported for the temperature range of 0–200°C [35].

Table 2
DSC results and calculated data obtained from superabsorbent micro-synthesis at various temperatures (Monomer concentration of 38.48 wt%, initiator concentration 0.0805 wt%. All symbols are introduced in the footnotes of Table 1)

Temperature (°C)	IP (min)	WL_{IP} (wt%)	MCg (wt%)	te (min)	Te (°C)	WL_{Te} (wt%)	q_{instr} (cal/g)	$-Q_{water}$ (cal)	$-Q_{instr}$ (cal)	$-\Delta H_{Rxn}$ (kcal/mol)	ER (%)
70	20.4 [16.34][a]	7.20	41.46	2.00	71.14 [70.10]	0.73	− 37.24 [−6.5]	0.026	0.399	8.98	56.1
75	14.50	6.40	41.12	1.36	77.37	0.94	− 19.18	0.033	0.205	5.07	31.7
80	11.00	5.81	40.85	1.40	84.22	1.01	− 23.78	0.036	0.256	6.22	38.8
85	8.58	5.30	40.63	1.07	86.43	0.97	− 8.49	0.034	0.091	2.70	16.9
90	6.69 [3.80][a]	5.70	40.80	1.00	91.22 [NM][b]	1.67	− 6.24 [NM][b]	0.058	0.067	2.67	16.7
95	6.12 [3.04][a]	5.60	40.76	0.90	95.56 [NM][b]	1.77	NM [NM][b]	0.062	–	–	–

[a] Wide exotherm weak peaks before the main exotherm.

[b] Not measurable, since it is immediately followed by the endothermic peak.

According to the IP and WL_{IP} values in Table 1, for the low initiator concentration (longer IP), higher amount of water is expected to evaporate compared to the high initiator case (WL_{IP} values). On the other hand, various rates of evaporation were observed in the case of temperature variation (Fig. 1). For instance, the rate of water evaporation for the temperature 95°C is approximately two times faster than the corresponding value for the temperature 70°C. So, the rate of water evaporation is critically dependent on the set temperature (Fig. 1). This in turn affects the monomer concentration of the reacting medium much more stronger than in the case of initiator variation (compare MCg values of Tables 1 and 2). Changing the initial bath temperature resulted in simultaneous change in IP (Fig. 2) and also in rate of evaporation (Table 2, WL_{IP} values). In contrast, only the IP was changed and no appreciable change in the rate of evaporation was observed with the initiator series (Table 1, WL_{IP} values). The exothermic peak observed after each evaporation is a typical exothermic polymerization reaction and the area under the peak is indicative of the heat of the reaction.

4.2. A descriptive kinetic approach to the process phenomenology

Extent of reaction (ER) as an overall value of reaction advancement was calculated and included as the last column of Tables 1 and 2. It was obtained by dividing the ΔH_{Rxn} by the heat of polymerization of acrylic acid in aqueous solution at 74.5°C which is reported to be -16.0 kcal/mol [36] (No heat of polymerization was found to be reported for sodium acrylate aqueous solution or for acrylic acid at alkaline conditions). It is clear from ΔH_{Rxn} and ER values (Tables 1 and 2) that increasing the initiator concentration gives the same effect as increasing the temperature does, i.e. lower temperature or less initiation concentration results in longer IP, more and sudden heat evolved and higher ER resulted. This trend can be explained based on the polyperoxide radical formation (ROOM$^{\cdot}$, Eqs. (3) and (4)). The rate of polyperoxide chain formation (R_p) in terms of numbers of moles of monomer segments is given by an expression with a square root dependence on the concentration of initiator [37], assuming the steady-state kinetics.

$$R_p = k_3(ek_1[S_2O_8^{2-}]/k_4)^{1/2}[M] \qquad (11)$$

In this expression, the rate constants correspond to reactions (1), (3), and (4), and e is the efficiency of persulfate dissociation to generate active radicals. Reaction (4) is taken to be the slowest step in the propagation reaction. According to the equation, the polyperoxide would accumulate at a rate inversely proportional to the square root of the rate constant of polyperoxide radical formation (k_4). On the other hand, the degree of polymerization is reported by Flory to be as low as 10–40, due to the facile dissociation of peroxide (–O–O–) bond. Therefore, each peroxide link might be a potential source of free radicals for initiating polymerization. Thus, in less initiator concentration or at lower temperature, the overall concentration of initiation radicals would increase with time, leading to more polyperoxide and to a self-accelerating process. At some point, the concentration of initiating radicals might become high enough to enable significant amounts of normal polymerization to occur, resulting in gelation, rapid increase in viscosity, slowing of oxygen diffusion resulting in its less inhibition action, advancement of reaction, and rise in ΔH_{Rxn} and ER. As we observed in both bench [38] and industrial scale [39], at lower temperature and with lower initiator amount, a glassy state solid material having water content of 10 wt%, is obtained after the sudden heat release (usually referred to as runaway polymerization). This suggests the possibility that polymerization was brought to stop prematurely by the lack of monomer mobility. This reason as well as local high initiator concentration (before gelation time) leads to a lower molecular weight (MW) polymer after gelation according to the well-known relationship of MW $\propto [M]/[I]^{1/2}$. Higher sol content of the products [11] confirms this result. Inversely, with high initiator amount or at higher temperatures (less dissolved O_2 in the reaction mixture), the initiator dissociates faster, the polymerization starts sooner and less water loses due to shorter IP followed by gentle and less heat release, i.e. lower ΔH_{Rxn} and ER. The post-gelation product is in the form of a soft rubbery state and able to continue polymerizing to a higher polymerization degree, resulting in lower sol contents and higher degrees of swelling [11], in spite of the lower initial ER.

Another feature of the DSC thermograms is a bimodal behavior, especially in the case of temperature experiments (see Fig. 2). This observation is consistent with the bench [38] and industrial scale observations [39] in which there are two steps in polymerization. Polymerization starts when sufficient amounts of the initiator radicals are generated at fixed reactor temperature. Afterwards, the reaction exotherm persuades more initiator radicals to decompose, so that more polymerization becomes possible which is associated with stronger exotherm and more appreciable gel formation. In such cases, processes like chain transfer to polymer chain presumably becomes much more probable in the presence of the initial gel (can be assigned to the first exotherm peak). This perturbs the linearity of the polymer structure and in turn induces branching in the superabsorbent structure, which improves its swelling properties.

Increase in temperature removes dissolved oxygen from the reaction mixture, so decreased oxygen concentration results in shorter induction period which leads to proximity of the two possible exotherm peaks and suppresses the main exothermicity (Table 2). Such a phenomenon was observed in the case of high initiator concentration (Table 1, Expt. 8 and 9), which could presumably be attributed to lack of complete solubility of the initiator at its higher extremes.

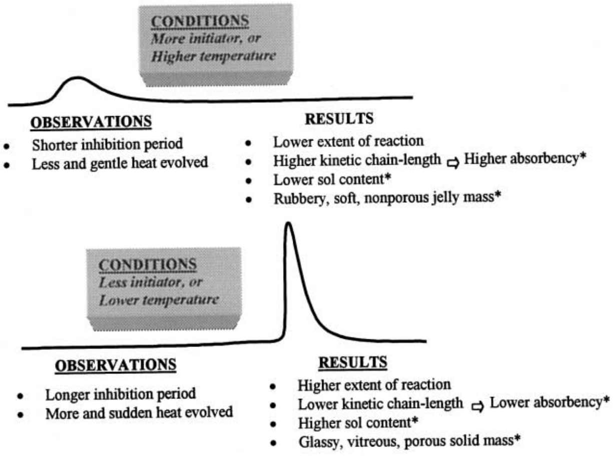

Scheme 2.

5. Conclusion

Regarding our previous investigations [6–12] of the solution process which is used industrially for producing superabsorbent polymers, it was found that unrestricted access of the reaction mixture to oxygen and unrestricted evaporative losses of water complicate the polymerization of the acrylic monomers and the swelling characteristics of the products. This complex behavior was mainly attributed to the existence of an IP, which was followed by the onset of rapid, apparently normal polymerization.

The existence of an IP in bench-scale was approved with the DSC data, in which normal polymerization could be started after a definite time. Moreover, a sudden rise in the viscosity of the reaction medium, which was already ascribed to the onset of the normal polymerization, was also cleared through the DSC studies as well. Scheme 2 shows illustratively the main results of these studies (Illustrative DSC thermograms were compared in terms of initiator and temperature variations as well as their effects on the course of polymerization. (*) Results taken from bench-scale experiments [11].)

Polymerization at lower temperatures and lower initiator concentrations favors longer IPs and vice versa. Longevity of the IP results in much more access to the atmospheric oxygen that in turn changes the polymer composition and its swelling properties. This means molecular oxygen can take part in the reaction and plays a role of unwanted comonomer. On the other hand, polymerization at higher initiator concentration and temperature presumably results in heterogeneity in the final product as DSC data shows a bimodal behavior in heat process during the synthesis.

Finally, it should be pointed out that the quantitative figures for the gelation time and exotherm, heat of reaction, and ER measured through DSC studies cannot necessarily be compared with bench-scale experiments without approximation, since the mass of the reaction for the latter case is about 1000 times bigger than that of the micro-scale reactor, and thus the surface to volume ratio of the two reactors are quite different. However, the overall semi-quantitative figure presented here can logically lead to a better understanding of the most important phenomena in the course of the synthesis of a superior hydrogel, i.e. superabsorbent.

References

[1] Buchholz FL. Trends Polym Sci 1994;2(8):277.
[2] Trijasson P, Pith T, Lambla M. Makromol Chem, Macromol Symp 1990;35/36:141–69.
[3] Buchholz FL. In: Buchholz FL, Graham AT, editors. Modern superabsorbent polymer technology. New York: Wiley-VCH, 1998. Chapter 7.
[4] Kazanskii KS, Dubrovskii SA. Adv Polym Sci 1992;104:97–133.
[5] Po R. J Macromol Sci, Rev Macromol Chem Phys 1994;C34(4):607–62.
[6] Askari F, Nafisi S, Omidian H, Hashemi SA. J Appl Polym Sci 1993;50:1851–5.
[7] Omidian H, Hashemi SA, Askari F, Nafisi S. Iran Polym J 1994;3(2):115–9.
[8] Omidian H, Hashemi SA, Askari F, Nafisi S. J Appl Polym Sci 1994;54:241–9.
[9] Omidian H, Hashemi SA, Askari F, Nafisi S. J Appl Polym Sci 1994;54:251–6.
[10] Omidian H, Hashemi SA, Sammes PG, Meldrum I. Polymer 1998;39(26):6697–704.
[11] Omidian H, Hashemi SA, Sammes PG, Meldrum I. Polymer 1998;39(15):3459–66.
[12] Omidian H, Hashemi SA, Sammes PG, Meldrum I. Polymer 1999;40:1753–61.
[13] SRI International and Nonwoven Industry, August 1989.
[14] Khanna YP, Taylor TJ. Polym Engng Sci 1987;27(10):764–71.
[15] Kamal MR, Sourour S. Polym Engng Sci 1973;13(1):59–64.
[16] Barton JM. Adv Polym Sci 1985;72:111–64.
[17] Ghaemy M, Khandani MH. Iran Polym J 1997;6(1):5–17.
[18] Gualpa MC, Riccardi CC, Vazquez A. Polymer 1998;39(11):2247–53.
[19] Han S, Kim WG, Yoon HG, Moon TJ. J Polym Sci, Polym Chem Ed 1998;36:773–83.
[20] Corcuera MA, Mondragon I, Riccardo CC, Williams RJJ. J Appl Polym Sci 1997;64:157–66.
[21] Salla JM, Ramis X. Polym Engng Sci 1996;36(6):835–51.
[22] Muzumdar SV, Lee LJ. Polym Engng Sci 1991;31(23):1647–56.
[23] Matuana LM, Riedel B, Barry AO. Eur Polym J 1993;29(4):483–90.
[24] Lee JH, Lee JW. Polym Engng Sci 1994;34(9):742–9.
[25] Liaw D-J, Shen W-C. Polym Engng Sci 1994;34(16):1297–303.
[26] Chu F, Mckenna T, Lu Sh. Eur Polym J 1997;33(6):837–40.
[27] Delgano R, Mcneill DM, Hawley MC. Polym Engng Sci 1994;34(9):734–41.
[28] Huang C-W, Sun Y-M, Huang W-F. J Polym Sci, Polym Chem Ed 1997;35:1873–89.
[29] Hernandez-Sanchez F, Vazquez-Torres H. J Polym Sci, Polym Chem Ed 1990;28:1579–92.
[30] Guida G, Pochini I, Nicolais L. J Mater Sci, Mater Med 1997;8(2):75–83.
[31] Chen J, Zhao Y. J Appl Polym Sci 1999;74:119–24.
[32] Chen J, Zhao Y. J Appl Polym Sci 2000;75:808–14.
[33] Barnes CE. J Am Chem Soc 1945;67:217.
[34] Bamford CH. Encyclopedia of polymer science and engineering, vol. 13. New York: Wiley, 1988. p. 762.

[35] Lide DR, editor. Handbook of chemistry and physics 74th ed. Boca Raton, FL: CRC Press, 1993. p. 6–10.
[36] Busfield WK. In: Brandrup J, Immergut EH, editors. Polymer handbook, 3rd ed. New York: Wiley, 1989. p. II/298.
[37] Flory PJ. Principles of polymer chemistry. Ithaca, NY: Cornell University Press, 1953 p. 114.
[38] Omidian H. Research documents on acrylic-based superabsorbent polymers. Report no. 2. Iran Polymer Institute, 1999.
[39] Omidian H. Technical documents of Nava-Baspar Chemical Company (leading Iranian superabsorbent manufacturer). Report no. 2. 1999.